

Chapter 1

Introduction

1.1 Sketch of molecular electronics

The idea of utilizing single molecules as functional devices in electrical circuits was introduced in a pioneering work by Aviram and Ratner [2]. Their 1974 theoretical paper may rightly be considered the foundation of the field called *molecular electronics* [3–7]. At the time of its publication, their envisioned molecular rectifier was mainly a gedanken experiment, as experimental techniques for realizing such single-molecule devices were still lacking.¹ Yet, a main motivation for this venture into the world of electronic transport at the nano- and molecular scale was, and still remains to be, a technological one: the anticipated limits of semiconductor-based microelectronics.

Since the invention of the transistor by Shockley, Bardeen, and Brattain in 1947 (Nobel prize 1956), the progress in constructing ever faster and more powerful computers has heavily relied upon technological advances in decreasing the structure sizes on semiconductor microchips. This miniaturization process is described remarkably well by the empirical observation known today as “Moore’s law” [8], stating that the structure size is reduced roughly exponentially as a function of time. With this relation, Moore’s law evidently predicts its own breakdown in the not too far future, for three reasons: (i) Miniaturization will cause increasing technological problems, such as the question of sufficiently efficient heat dissipation. (ii) Further reduction of structure sizes may pose the economical question of profitability. (iii) Finally, quantum physics sets a fundamental barrier to size reduction.

Ever since the experimental advance which demonstrated the feasibility of single-molecule devices [9], molecular electronics has been perceived as one possible route to accomplish another technological leap in miniaturization. The relevant orders of magnitude in size are illustrated in Fig. 1.1. Despite the impressive recent experimental and theoretical progress in measuring and calculating transport through molecular junctions, which we will discuss below, it is still too early to assess the practicability of molecular electronics in its technological sense. It is safe to say that major experimental breakthroughs will be required to wire not only a single molecule, but a huge number² of molecules in an

¹In fact, Aviram and Ratner explicitly point out in their paper that “A large number of material and synthesis problems must, clearly, be overcome before such a molecular electronic device can be tested in the laboratory.”

²State of the art microprocessors incorporate of the order of 10^8 transistors.

organized network [3].

However, independent of the challenge of concrete applications, molecular electronics has crystallized into a flourishing field of research at the interface between experimental and theoretical physics and chemistry. In its pursuit of understanding electronic transport at the molecular scale, it poses physics questions of fundamental importance. In a natural way, it continues the endeavor of clarifying transport phenomena in ever smaller structures, which has seen immense successes in the field of mesoscopic physics during the last decades [10,11]. In fact, transport through single molecules has turned out to show significant similarities to transport in more conventional nanostructures such as semiconductor quantum dots, including effects like Coulomb blockade [11,12] and the Kondo effect [13,14]. In the following, we proceed to give a representative (but by no means exhaustive) cross section of the current experimental and theoretical status of molecular electronics.

1.1.1 Experiments

To a considerable extent, the thriving interest in transport through molecular junctions in recent years is owed to the ingenious experimental schemes which have been developed for the setup of single-molecule devices. A number of groups have impressively demonstrated that such devices can actually be realized, and experimental control over these systems is rapidly improving. The most popular experimental techniques create two closely spaced electrodes, most frequently made of noble metals like gold or platinum, by the use of breakjunctions [15–17] or electromigration [18]. The molecule may or may not be chemically bound (e.g. by thiol groups) to the electrodes. A recent alternative method first attaches the molecule to gold clusters via thiol groups before maneuvering (using ac-fields) the resulting conglomerate towards two microfabricated electrodes [19]. A further intriguing direction is the use of wet molecular junctions, where the molecule is immersed in an electrolytic environment [20]. Another powerful method employs a scanning-tunneling-microscope (STM) tip as an electrode for measuring the current through a molecule, which rests on a substrate [21]. The resulting two prototypical types of single-molecule devices are schematized in Fig. 1.2.

To date, a large variety of molecules ranging from H_2 [22] to DNA [23] have been investigated experimentally in two-terminal [22–24] and three-terminal [25–31] molecular devices. The inexhaustible pool of different molecules to choose from reflects a major appeal of molecular electronics: Chemistry allows the targeted design of specific molecules, tailoring them for a certain functional behavior in the resulting device. Following this path, experiments have demonstrated rectification effects in molecular monolayers [32–34] and for single molecules [35], as well as molecular memory devices [36] and switches [37]. Many of today’s experiments observe effects familiar from conventional nanostructures such as quantum dots, especially in setups that include a gate electrode. Pertinent examples are the Coulomb blockade which arises due to the large charging energy of nanostructures [27, 29], as well as the Kondo effect [29,38]. Due to the small size of molecules, the Kondo effect in these systems persists to rather high temperatures [29]. It has been argued that Coulomb-blockade physics, via charging fluctuations of nearby traps, is also at the origin of temporal fluctuations in the measured current-voltage (IV) characteristics [19].

A prime qualitative difference between transport through single molecules as opposed to

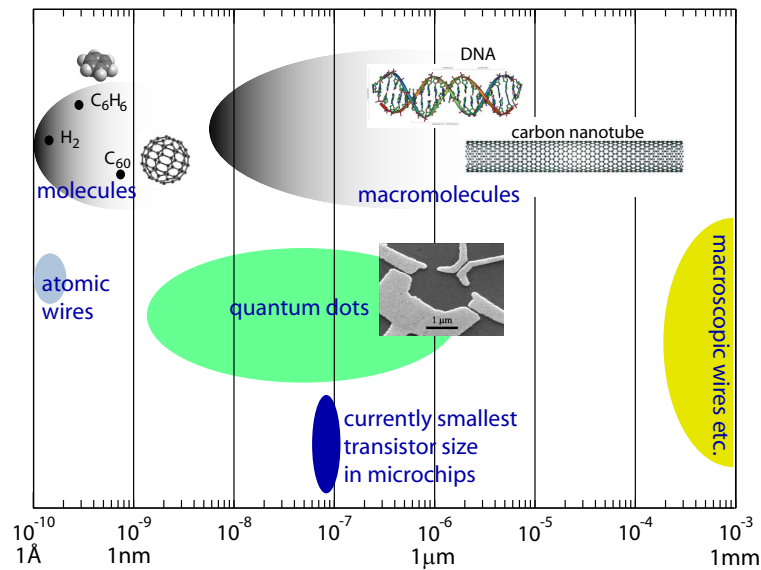


Figure 1.1: Electronic transport: Illustration of length scales. (Molecular sizes are based on nuclear distances. The quantum-dot figure is taken from the website of C. Schönberger's group in Basel.)

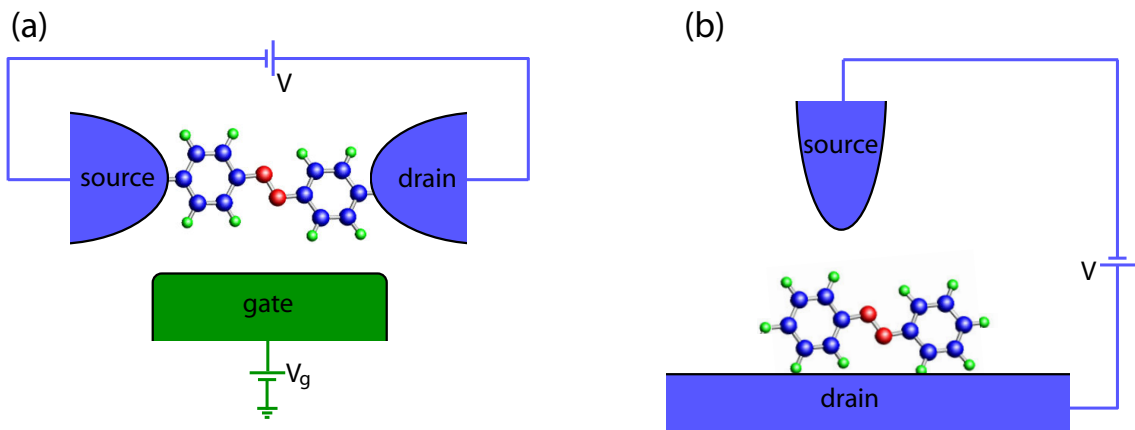


Figure 1.2: Prototypical single-molecule devices. (a) Schematic setup of a three-terminal single-molecule device. The molecule is coupled to two metallic source and drain electrodes. Applying a bias voltage V drives an electric current across the molecule. A third electrode, the gate, is capacitively coupled to the junction and allows for a tuning of orbital energies via the gate voltage V_g . (b) Schematic STM setup for measuring transport through a single molecule. The molecule is located on a conducting surface, the second electrode is realized by an STM tip.

transport through conventional nanostructures lies in the coupling of the electronic degrees of freedom (responsible for transport) to few well-defined collective modes such as local spins or molecular vibrations (phonons). This type of coupling is specific to molecules and leads to novel effects which transcend the findings for transport through quantum dots. Intriguingly, the coupling to spin degrees of freedom, confirmed in a recent experiment by Heersche et al. [39], even opens up the possibility of combining the fields of molecular electronics and spintronics.

The main focus of this work will be the coupling between electrons and vibrations. A prominent effect of this electron-phonon coupling is the appearance of vibrational sidebands in the current-voltage characteristics. These are observed at large bias voltages, comparable to or larger than typical phonon frequencies. While the basic phenomenon has been known for a number of decades [40–42], current interest in the context of single-molecule junctions started with the work of Park et al. [26] on a C_{60} molecule located in between two metallic leads. In their case, center-of-mass oscillations of the molecule are responsible for the observed sidebands in the IV characteristics, see Fig. 1.3.

In the meantime, vibrational features have been observed in transport in a wide variety of molecules, ranging from hydrogen H_2 [22] to larger conjugated molecules [21]. Depending on the system, vibrations appear in the IV characteristics as steps or kinks [43]. Typically, molecules more strongly coupled to the leads (as for example in STM experiments where the molecule is lying on the substrate) will exhibit kinks in the IV characteristics [21]. By contrast, steps in the IV characteristic are observed for weakly coupled molecules (as for example in breakjunction experiments without chemical bond between electrode and molecule) [26, 31].

An important parameter in single-molecule junctions is the vibrational relaxation rate. For some systems, relaxation times can be as large as 10ns (measured for suspended nanotubes) [44]. Thus, these times can be comparable or longer than the time between two consecutive electrons traversing the molecule, which is of the order of 100ps (0.1ps) for a current of 1nA ($1\mu A$). As a result, in the intriguing regime of slow vibrational relaxation (or large currents), the current is expected to drive the molecular vibrations far out of equilibrium, see e.g. Ref. [45] and Chapter 6. Such nonequilibrium vibrations have so far been observed directly in at least one experiment as *absorption* satellites of Coulomb blockade peaks [44].

1.1.2 Theory

The theoretical description of transport through single molecules to date essentially rests on two pillars which are at present somewhat disconnected.

Density Functional Theory

One approach uses density functional theory [46, 47] to obtain a detailed account of the molecular orbitals including parts of the electrodes, see e.g. [48–50]. In a second step, the Kohn-Sham potentials of density functional theory are used to set up a (single-particle) transport problem in the spirit of Landauer. While there are impressive successes, differences between experiment and this “ab-initio” theory can be as large as several orders of magnitude [51]. Discrepancies between theory and experiment are particularly pronounced

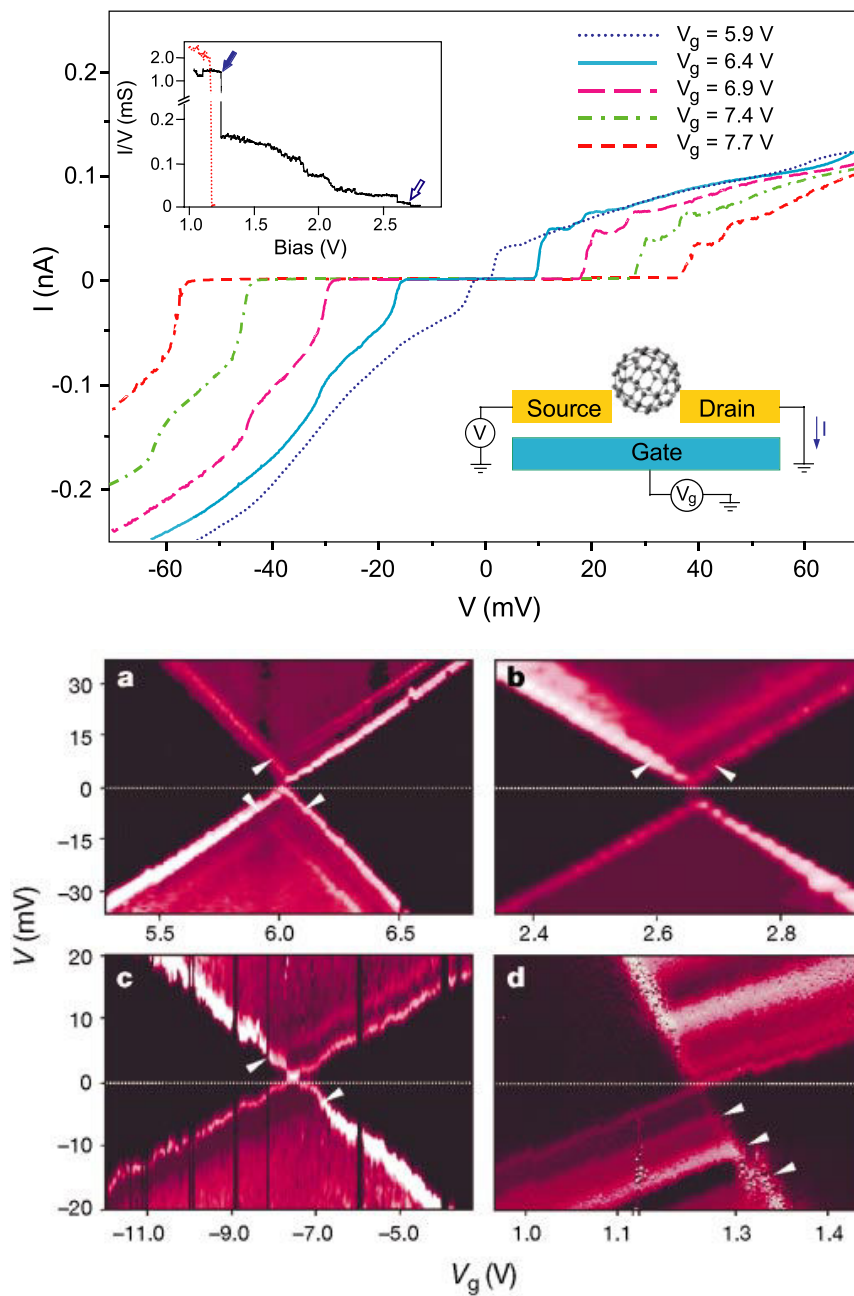


Figure 1.3: Experimental data by H. Park et al. for electronic transport through a single C₆₀ molecule coupled to gold electrodes. Upper panel: Current-voltage characteristics for a C₆₀ transistor, exhibiting a set of steps due to center-of-mass oscillations of the molecule between the leads. The inset shows the current while opening the junction by electromigration. Lower panel: Differential conductance for four different devices as a function of gate and bias voltage. White arrows mark the positions of vibrational sidebands. *These figures are taken from Reference [26].*

for small conjugated molecules. It is important to realize that the use of density functional theory for transport is ultimately an uncontrolled (though often useful) approximation as there is no theorem underlying the treatment of nonequilibrium transport on the basis of the Kohn-Sham orbitals. An additional difficulty is the inclusion of coupling to molecular vibrations as well as electronic correlations (leading, e.g., to the Kondo effect) within density functional theory. There are some efforts under way to improve this situation within the context of time-dependent density functional theory [52–55].

Models for electronic transport through nanostructures

An alternative approach starts from models of electronic transport through nanostructures, see e.g. [45, 56–61]. This type of approach finds its justification in the fact that experiments on molecular junctions exhibit several phenomena which are familiar from quantum dots. In extension to quantum-dot physics it enables the investigation of additional degrees of freedom including, e.g., mechanical, and magnetic degrees of freedom leading to phonon and spin dynamics. In addition, such models can in principle be treated *systematically* in a variety of transport regimes, including the coupling to molecular vibrations and electronic correlation effects. The present work will follow this type of approach.

Recently, there has been considerable theoretical effort to calculate current-voltage characteristics of single-molecule devices within such transport models. Effects such as negative differential resistance (NDC) [56–58], influences of phonons and dissipation [45, 58–62], as well as noise spectra [45] have been studied intensely. In addition, several studies have suggested mechanisms for developing diodes [63] and switches [64]. In the following section we develop and explain the theoretical model which forms the basis for our work in subsequent chapters.

1.2 Generic model

We consider a three-terminal single-molecule device, consisting of a molecule coupled to two metallic leads serving as source and drain electrode, respectively. The third electrode only influences the molecule by electrostatic interaction and acts as a gate electrode. This setup is schematically depicted in Fig. 1.2(a). As discussed in Section 1.1.1, experiments have shown the significance of Coulomb blockade and Kondo effect for such molecular devices [29, 38]. This input provides the essential motivation for the modeling of the system.

In theoretical studies, the Anderson-Holstein Hamiltonian has emerged as a natural starting point for analyzing transport through vibrating molecules [41, 42, 45, 60, 65]. This Hamiltonian provides the minimal model which encapsulates Coulomb blockade, the Kondo effect, as well as vibrational sidebands [45, 60, 66, 67]. The key features of the model are schematized in Fig. 1.4. Several assumptions and simplifications enter this model:

- (i) Transport is assumed to be dominated by tunneling through one spin-degenerate orbital of the molecule with single-particle energy ε_d . Due to Coulomb interaction, double occupation of the orbital is associated with an additional charging energy $U > 0$.

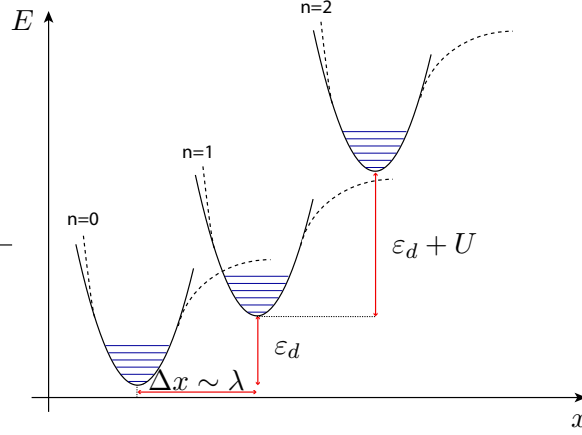


Figure 1.4: Potential surfaces corresponding to the Anderson-Holstein Hamiltonian of a molecule featuring a single, spin-degenerate electronic orbital coupled to a single vibrational mode. The model Hamiltonian approximates the potential surfaces by a harmonic-oscillator potential. The electron-phonon coupling, parameterized by the coupling strength λ , corresponds to a charge-dependent x -shift of the potential surfaces.

- (ii) One mode of molecular vibrations with frequency ω_0 is taken into account within the harmonic approximation.
- (iii) In addition, electronic relaxation is taken to provide the shortest time scale in the problem, so that the metallic electrodes are described by Fermi seas in thermal equilibrium at all times. Its second important effect is to provide a dephasing mechanism in the transfer of electrons. Dephasing plays a crucial role in the issue of coherent versus incoherent transport, see e.g. the discussion in References [68–70]. Specifically, in the absence of dephasing, transport is fully coherent and real occupation of the molecule cannot occur. By contrast, strong dephasing, which is the realistic scenario for transport through molecules considered in this work, gives rise to incoherent processes with a finite residence time of electrons on the molecule (such as sequential tunneling, see below).

These ingredients result in the Anderson-Holstein Hamiltonian $H = H_{\text{mol}} + H_{\text{leads}} + H_{\text{mix}}$ with

$$H_{\text{mol}} = \varepsilon_d n_d + U n_{d\uparrow} n_{d\downarrow} + \hbar\omega_0 b^\dagger b + \lambda \hbar\omega_0 (b^\dagger + b) n_d \quad (1.1)$$

describing the electronic and vibrational degrees of freedom of the molecule,

$$H_{\text{leads}} = \sum_{a=L,R} \sum_{\mathbf{p},\sigma} (\varepsilon_{\mathbf{p}} - \mu_a) c_{a\mathbf{p}\sigma}^\dagger c_{a\mathbf{p}\sigma} \quad (1.2)$$

the noninteracting leads, and

$$H_{\text{T}} = \sum_{a=L,R} \sum_{\mathbf{p},\sigma} \left(t_a c_{a\mathbf{p}\sigma}^\dagger d_\sigma + \text{h.c.} \right) \quad (1.3)$$

the tunneling between leads and molecule.

1.2.1 Explanation of the Anderson-Holstein model

In the following, we give a detailed explanation of the Anderson-Holstein Hamiltonian, starting with the simple contribution H_{leads} for the noninteracting leads. The operator $c_{a\mathbf{p}\sigma}$ ($c_{a\mathbf{p}\sigma}^\dagger$) annihilates (creates) an electron in lead a ($a = L, R$) with momentum \mathbf{p} and spin projection σ . Throughout this work, we assume that the left and right leads consist of the same material, resulting in identical band structures. Typically, the energy range involved in transport is small compared to the width of the conduction band. Accordingly, the so-called wide-band limit can be applied, i.e. we may approximate the density of states of the leads by a constant,

$$\rho(E) = \sum_{\mathbf{p}} \delta(E - \epsilon_{\mathbf{p}}) \approx \text{const.} \quad (1.4)$$

For vanishing bias voltage $V = 0$, both leads assume the same Fermi energy, which we define as the zero-point of our energy scale. At finite bias, the left and right chemical potentials $\mu_{L,R}$ are shifted and their difference is fixed by $\mu_L - \mu_R = eV$. The exact voltage splitting between the left and right junction depends on details of the junction capacitances – a fact well-known in the context of conventional quantum dots [11]. In the general case, the voltage splitting may be described by a capacitance-related splitting parameter $0 \leq \eta \leq 1$ such that

$$\mu_L = \eta eV, \quad \mu_R = (1 - \eta) eV. \quad (1.5)$$

We now turn to the discussion of the molecular and tunneling terms, H_{mol} and H_{T} . The operator d_σ (d_σ^\dagger) annihilates (creates) an electron with spin projection σ on the molecule, and $n_{d\sigma} = d_\sigma^\dagger d_\sigma$, $n_d = \sum_\sigma n_{d\sigma}$ denote the corresponding spin-resolved and total occupation-number operators. The orbital one-particle energy ε_d is measured with respect to the zero-bias Fermi energy, and it may be tuned by applying a voltage V_g to the gate electrode, $\varepsilon_d \rightarrow \varepsilon_d - eV_g$. Throughout the text, we will absorb the gate voltage into the parameter ε_d , and treat them on the same footing. It is useful to note that the case of asymmetric voltage splitting, i.e. $\eta \neq 1/2$, can always be compensated for by tuning the gate voltage. Thus, we may restrict our discussion to the case of symmetric voltage splitting $\mu_{L,R} = \pm eV/2$ in the following. The actual transfer of electrons between the leads and the molecule is described by the tunneling Hamiltonian H_{T} . The strength of this coupling is parameterized by the tunneling matrix elements t_a .

Vibrational excitations with energy $\hbar\omega_0$ are annihilated (created) by b (b^\dagger). The coupling between vibrational and electronic degrees of freedom is described by the term $\lambda\hbar\omega_0 n_d (b^\dagger + b)$. The nature of this coupling term is elucidated by the Lang-Firsov canonical transformation [71], which we review in Appendix A.1. The transformation corresponds to a basis change to polaron-type quasi-particles – electrons surrounded by clouds of vibrations. The transformed Hamiltonian reads $H' = H'_{\text{mol}} + H'_{\text{leads}} + H'_{\text{T}}$ with $H'_{\text{leads}} = H_{\text{leads}}$, and

$$H'_{\text{mol}} = (\varepsilon_d - \lambda^2 \hbar\omega_0) n_d + (U - 2\lambda^2 \hbar\omega_0) n_{d\uparrow} n_{d\downarrow} + \hbar\omega_0 b^\dagger b, \quad (1.6)$$

$$H'_{\text{T}} = \sum_{a=L,R} \sum_{\mathbf{p},\sigma} \left[t_a e^{-\lambda(b^\dagger - b)} c_{a\mathbf{p}\sigma}^\dagger d_\sigma + \text{h.c.} \right]. \quad (1.7)$$

Hence, beyond the elimination of the electron-phonon coupling term $\lambda\hbar\omega_0 n_d (b^\dagger + b)$, the central consequences of the transformation are:

- (i) In the new Hamiltonian, the presence of electron-phonon coupling is reflected by an additional shift operator in the tunneling matrix elements, $t_a \rightarrow t_a e^{-\lambda(b^\dagger - b)}$.
- (ii) The orbital energy and the charging energy get renormalized, $\varepsilon_d \rightarrow \varepsilon_d - \lambda^2 \hbar \omega_0$ and $U \rightarrow U - 2\lambda^2 \hbar \omega_0$ (*polaron shift*).

In the following, we will proceed with the transformed Hamiltonian and drop all primes.

The transformation allows for a transparent interpretation of the electron-phonon coupling. The charging of the molecule by additional electrons requires a relaxation of the molecular structure. In particular, the equilibrium distances between nuclei of the molecule differ between charge states. This physics is reflected in a normal-coordinate shift of the potential surface minimum, see Fig. 1.4. In the transformed Hamiltonian, this is encoded by the translation operator in the tunneling matrix elements. The strength of the electron-phonon coupling is characterized by the dimensionless coupling parameter λ , which determines the magnitude of the potential-surface shift in units of the harmonic-oscillator length³ $\ell_{\text{osc}} = \sqrt{\hbar/M\omega_0}$. The precise relation between shift distance Δx and λ is given by $\Delta x = \sqrt{2}\lambda\ell_{\text{osc}}$.

1.2.2 Regimes of the Anderson-Holstein model

There are four different energy scales relevant to the analysis of transport in the Anderson-Holstein model: the phonon energy $\hbar\omega_0$, the tunneling-induced level width $\Gamma = 2\pi \sum_a \rho |t_a|^2$, and the energy scales set by the Kondo temperature T_K and by the ambient temperature T . Additional important parameters are the strength of the vibrational relaxation,⁴ the electron-phonon coupling λ , and the coupling asymmetry Γ_L/Γ_R . As a result of this multitude of energy scales and relevant parameters, the Anderson-Holstein model incorporates an astonishing wealth of qualitatively different transport regimes.

It is beyond our scope to give an exhaustive classification of all different regimes, and we emphasize that the investigation of the Anderson-Holstein model and the development of controlled approximations in certain regimes is still an active field of research to date. For a characterization of the regimes covered in this work, we discuss the two fundamental ratios $\hbar\omega_0/\Gamma$ and $k_B T/\Gamma$. The significance of the latter ratio can be understood in an easy way when considering the exactly solvable case of the resonant-level model.⁵ For $k_B T/\Gamma \gg 1$, the width of the conductance peak is determined by temperature, and transport can be captured appropriately by approximating the spectral function by a Dirac- δ function. In the opposite limit, $k_B T/\Gamma \ll 1$, the width of the conductance curve is fixed by the tunneling-induced level width Γ , and the conductance measurement probes the actual Lorentzian shape of the spectral function. Similarly, the limits $\hbar\omega_0/\Gamma \gg 1$ and $\hbar\omega_0/\Gamma \ll 1$ result in different physics. If the phonon energy is large compared to the level width, then different vibrational states do not get mixed, and the system completes many oscillation cycles between tunneling

³The harmonic-oscillator length is a measure of the spatial extent of the vibrational ground state, $\ell_{\text{osc}} = \sqrt{\langle x^2 \rangle_0}$.

⁴Such relaxation of vibrational excitations will always be present in a real system, and relevant mechanisms include the interaction between the molecule and the substrate, radiation, and the coupling to other vibrational modes.

⁵By this, we mean a noninteracting electronic level coupled to two electrodes, which can be solved in a simple one-particle scattering approach.

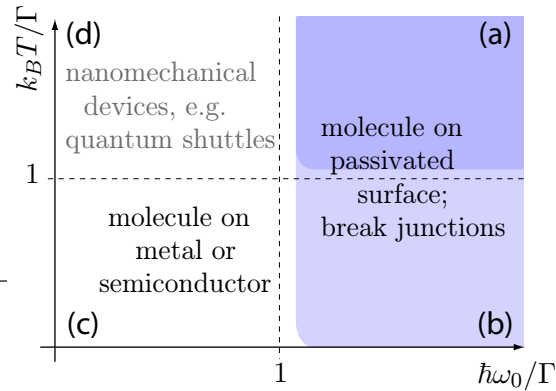


Figure 1.5: Different regimes of the Anderson-Holstein Hamiltonian as a function of the ratios $k_B T/\Gamma$ and $\hbar\omega_0/\Gamma$. Colored regions mark the regimes discussed in this work. Exemplary references for the different regimes are (a) Refs. [45, 60, 72], (b) Refs. [45, 60, 66], (c) Refs. [73, 74], and (d) Refs. [75, 76]

events. On the other hand, for phonon energies small compared to the level width, a strong mixing between vibrational states occurs and coherences between them must be taken into account. A scenario typical of this limit is the case of quantum shuttling in nanomechanical devices [75, 76].

The majority of our results is obtained in the *weak-tunneling limit*, defined by $\Gamma \ll \hbar\omega_0, k_B T$. This limit is applicable to single-molecule devices which are weakly coupled to the source and drain electrodes. This is the case, e.g., in setups without chemical bonds between the molecule and the leads [26]. Weak coupling may also be realized in situations where bonds are present but do not feature a well-conducting orbital between the leads and central conducting parts of the molecule, especially π -conjugated units. In this regime, the tunneling Hamiltonian H_T can be treated in a systematic perturbation theory, and the calculation of transport characteristics may be carried out within the framework of rate equations. We give an account of this formalism in Chapter 2.

1.2.3 Extensions of the model

The Anderson-Holstein Hamiltonian captures the central experimental findings of Coulomb blockade, Kondo effect, and vibrational sidebands. The major advantage of this model is its relative simplicity, which in many situations allows for controlled approximations and an essentially *analytical* treatment. It should be stressed however that a truly *quantitative* description of a specific single-molecule device will generally require extensions of the model. Various such extensions have been addressed in the literature, and we will discuss some of them in the course of this work.

A particularly important extension regards the influence of vibrational relaxation, driving the molecular phonon distribution towards the thermal equilibrium. This effect can be described either in the spirit of the Caldeira-Leggett model [77], see e.g. Ref. [72], or by a relaxation-time approximation on the level of the rate equations, see Chapter 2. For molecules with relatively small dissociation energies or, generally, in nonequilibrium situation involving highly excited vibrational states, transport may also probe the anharmonicity

of the underlying molecular potential surface. In this case, generalizations going beyond the harmonic approximation are essential. Such effects may be discussed in the context of a Morse-potential model, see Chapters 5 and 6. Further extensions, which may be relevant for a modeling of real single-molecule transistors, include the dependence of the vibrational frequency on the molecular charge state, see Chapter 5 and Ref. [65], the competition of several molecular orbitals [78], and the involvement of several vibrational modes.

The Anderson-Holstein Hamiltonian does not include possible magnetic degrees of freedom of the molecule. Several recent studies have investigated the effects of a localized magnetic moment, and have found interesting effects such as a novel type of spin blockade [79–81]. However, in these papers the possible influence of molecular vibrations has been neglected so far. A very promising direction for future research consists of the consideration of the interplay between magnetic and vibrational degrees of freedom, which may give rise to new collective transport effects.

1.3 Overview of the thesis

The chapters of this thesis are organized as follows. In **Chapter 2** we develop the theoretical tools used most frequently throughout this work. In particular, we discuss the systematic perturbation theory in the tunneling, applicable in the weak-tunneling limit. Starting with the leading order, we explain the notion of *sequential tunneling* and describe how to calculate the relevant rates. The presence of molecular vibrations leads to the emergence of *Franck-Condon matrix elements*, and we illustrate their qualitatively different behavior for weak, intermediate, and strong electron-phonon coupling. Proceeding with the next-to-leading order, we derive the rates for *cotunneling* processes. The complication of diverging Fermi's golden rule expressions is discussed in detail, and a well-defined regularization procedure is established to extract the correct cotunneling contributions. In the final two parts of Chapter 2 we demonstrate how these transition rates are used as input for the *rate equations*, which determine the occupation probabilities of the system, and we show how crucial transport quantities such as the *stationary current* and the *noise spectrum* are calculated.

All central results of this thesis are related to the coupling between electrons and phonons, and thus can be traced back to one of the two main consequences of the electron-phonon coupling. The presence of Franck-Condon (FC) matrix elements due to the modified tunneling matrix elements will be investigated in detail in Chapters 3 through 7. In **Chapter 3** we start our study with the regime of *strong electron-phonon coupling*, characterized by large displacements between the molecular potential surfaces. In this case, the characteristics of the FC matrix elements leads to a low-bias current suppression, termed *Franck-Condon blockade*, which reflects the exponentially small overlap between vibrational states in the vicinity of the ground state. Going beyond the mere calculation of *IV* characteristics by Monte-Carlo simulations and computation of the current shot noise, we find that for weak vibrational relaxation, transport is dominated by a *hierarchy of self-similar electron avalanches*. This unusual transport mode drastically affects the current shot noise, leading to *strongly enhanced Fano factors* and a *power-law behavior of the noise power spectra*. The fact that transport predominantly proceeds in a unidirectional fashion allows us to develop an analytical theory for avalanche transport. In addition to current and noise, we

investigate the *full counting statistics*, and we show that the presence of avalanches leaves distinctive fingerprints in the form of strongly non-Ohmic distributions.

The results of Chapter 3 are derived within the sequential-tunneling approximation. In **Chapter 4** we extend our investigation of the FC-blockade regime by considering *cotunneling* processes. This is motivated by the insight that the involvement of excited virtual phonon states in higher-order processes leads to a significant reduction in FC suppression. Due to this increased overlap of vibrational states, cotunneling is found to *dominate* the linear conductance and nonlinear *IV* in the low-bias regime. Nevertheless, our results for *IV* characteristics and noise spectra show that cotunneling primarily affects the sequential waiting periods and that avalanches involving real phonon excitations persist. Intriguingly, beyond these modifications cotunneling also gives rise to effects entirely missed by the sequential approximation. In particular, we find that for weak vibrational relaxation inelastic cotunneling results in the appearance of *absorption-induced vibrational sidebands* inside the conventional Coulomb-blockade regime. In addition, the peculiar situation of cotunneling rates dominating over sequential rates leads to *current telegraph noise*, associated with enhanced Fano factors independent of the relaxation rate.

Chapter 5 presents an excursion beyond the Anderson-Holstein model, where we investigate the effects of a *charge dependence of the vibrational frequency* and of *anharmonic potentials*. These generalizations of our basic model are expected to be relevant for a more accurate description of real single-molecule devices, where different shapes of the molecular potential surface for the neutral and ionized molecule as well as the presence of a dissociation threshold cannot be avoided. For strong vibrational relaxation, the *non-equidistant spacing of vibrational sidebands* signals the involvement of different vibrational energy scales. Interestingly, for weak relaxation we find that the resulting incommensurability of vibrational energies is directly reflected in the *IV* by a *splitting of vibrational sidebands* into a multitude of subbands. At finite temperatures, this represents an additional *effective broadening mechanism* for vibrational sidebands.

The journey towards capturing the properties of real single-molecule devices is continued in **Chapter 6**, where we analyze the effects of *weak electron-phonon coupling* and its implications for the possible *dissociation of molecules* (and hence the destruction of the device). We start our investigation on the basis of the Anderson-Holstein model, showing that the characteristics of FC matrix elements at weak coupling leads to phonon dynamics described by a *generalized diffusion process*. Remarkably, the resulting nonequilibrium phonon distributions are found to become wider with decreasing electron-phonon coupling. By formulating a Fokker-Planck equation for the phonon distribution, we are able to extract analytical expressions for this distribution and conclude that its width *diverges with noninteger powers of the coupling* λ . This important result indicates that a perturbation theory in λ must be assessed with extreme care for fully developed nonequilibrium. Indeed, we find that the divergence is naturally cut off by the relaxation of vibrational excitations. By transferring these findings to an extended Morse-potential model, we show that weak electron-phonon coupling may lead to the dissociation of the molecule at hand, and we present results for the *mean dissociation rate*, obtained by Monte-Carlo simulations.

As is well-known from the Peltier-Seebeck effect in solid-state physics, electronic transport may not only be generated by the application of electric potential differences but also by temperature gradients. In **Chapter 7** we study this thermoelectrical effect in single-

molecule devices in the linear-response regime by calculating the *thermopower*. The thermopower has several appealing properties. First, it is nonzero only for broken particle-hole symmetry. Its sign indicates whether transport is dominated by electron or hole conduction, and thus reveals whether the tunneling involves the molecular *HOMO* or *LUMO*. In this regard, the thermopower provides information which *cannot* be extracted from the *IV* characteristics. Second, we find that the coupling to molecular vibrations leads to characteristic *sawtooth-like features* in the thermopower as a function of gate voltage. The important message of the chapter is that phonon excitations can be probed in a thermoelectric linear-response measurement. By contrast, the linear conductance does not access these excitations. Third, we note that the thermopower is a quantity which is remarkably *sensitive to cotunneling* and we explain how such higher-order processes modify the thermopower behavior.

While Chapters 3 through 7 mainly focus on the consequences of the FC matrix elements, in **Chapter 8** we turn to the investigation of the second consequence of the electron-phonon coupling: the *polaron-shift* of the charging energy U . This downward regularization may result in *effectively negative charging energies*, a scenario indeed observed for a variety of molecules in electrochemistry experiments. Negative charging energy leads to the preference of even-number occupation of the molecule. After developing an effective negative- U model for transport, we show that transport beyond the Kondo regime is dominated by *tunneling of electron pairs*. The two-particle nature of such pair-tunneling processes leads to transport characteristics profoundly different from the conventional Coulomb-blockade physics. In particular, we find that the width of the pair-tunneling conductance peak scales with temperature, but that its height is fixed to a constant value. Furthermore, the nonlinear *IV* characteristics reveal that pair tunneling in devices with asymmetric junctions causes *current rectification and gate-controlled switching*. Fingerprints of pair tunneling are also found in the zero-frequency noise, which exhibits super-Poissonian Fano factors due to the two-particle processes.

Interestingly, there is a close relationship between the negative- U and the conventional Anderson model. For the equilibrium situation, this was already pointed out in the 70s by Iche and Zawadowski [82] and further elucidated by Haldane [83]. In Chapter 8 we present an exact canonical transformation, the *particle-hole/left-right transformation*, which maps transport within the negative- U model to transport within the conventional Anderson model with an additional local Zeeman field. This mapping enables us to transfer results from the negative- U to the positive- U scenario, and vice versa. In particular, it allows for an *analytical understanding of the charge-Kondo effect*, which arises from the degeneracy of the empty and doubly-occupied molecular states.

In **Chapter 9** we give an comprehensive summary of the conclusions to be drawn from this thesis, and discuss interesting future research directions in the field of molecular electronics. The thesis closes with a number of **Appendices**, which have been separated from the text so not to disrupt the main line of thought with technical details. References to these appendices are given in the text in appropriate places.